

The first excited states of ${}^9\text{Be}$ and ${}^9\text{B}$

V.D. Efros¹⁾ and J.M. Bang²⁾

1) *Russian Research Centre "Kurchatov Institute", Kurchatov Square 1, 123182 Moscow, Russia*

2) *The Niels Bohr Institute, Blegdamsvej 17, DK-2100 Copenhagen, Denmark*

(December 2, 2024)

Abstract

It is derived that the $1/2^+$ first excited state of ${}^9\text{Be}$ is a virtual state with the energy of -23.5 KeV, while its partner in ${}^9\text{B}$ is a resonant state with a maximum in the peak at about 1.1 MeV, FWHM of 1.5 MeV, and complex energy of $0.6 - i0.75$ MeV. The derivation based on $N - {}^8\text{Be}$ effective potentials deduced from the data on the photodisintegration of ${}^9\text{Be}$. We also consider universal line shapes for excitation of virtual and resonant states decaying into two fragments, some general properties of virtual states, and the calculation of complex energy eigenvalues for resonant states.

PACS numbers: 21.10.Pc, 23.50.+z, 24.30.Gd, 27.20.+n, 03.65.Nk

I. INTRODUCTION

In the present work, we derive the properties of the first excited states of $A = 9$ nuclei. At low energy these nuclei provide a clean example of three-cluster systems with not easily distortable constituents thus serving as a testing ground for multicluster approaches both at the three-body [1] and nine-nucleon [2] level. A reliable information on the properties of these nuclei is therefore necessary. In the next section we elucidate the nature of the first excited state of ${}^9\text{Be}$, obtain its precise position, and investigate to what degree the shape of the line for its excitation is independent of the specific excitation process. In Sec. 3 the position and width of the first excited state of the ${}^9\text{B}$ nucleus are found. There exists a long-standing controversy concerning the properties of this state, as obtained both experimentally and theoretically, see [3,4]. In Sec. 4 our results are discussed along with those in the literature.

Our considerations on the shape of the line in Sec. 2 and 3 are of a rather general applicability. Additional general considerations used in the present $A = 9$ study are listed in Appendices. In Appendix A a formula expressing a residue at a virtual state pole in terms of a quadrature taken over the virtual state eigenfunction is given. In Appendix B it is shown that in a system with a long-range Coulomb repulsion low-energy virtual states cannot exist. In Appendix C the procedure we use to calculate complex eigenvalues corresponding to resonances is listed.

II. THE FIRST EXCITED LEVEL OF ${}^9\text{BE}$

We proceed from the dynamic input for the description of the system obtained in Ref. [5]. In that work, the ${}^9\text{Be}$ photodisintegration cross section has been constructed in the framework of the following model. The three-body $\alpha + \alpha + n$ representation of the system has been adopted. The ${}^9\text{Be}$ ground state wave function has been calculated from the three-body dynamic equation with $\alpha\alpha$ and αn potentials. The final continuum state has been chosen as a product of the intrinsic wave function of ${}^8\text{Be}$ and the $n - {}^8\text{Be}$ relative motion function. The latter wave function has been calculated from the Woods-Saxon potential whose parameters were determined by fitting to several radioactive isotope data. As explained in Ref. [5] in spite of the restricted form of the final state wave function the model provides approximately correct energy dependence of the cross section in the vicinity of the first excited state of ${}^9\text{Be}$. This occurs because of the strong inhibition of the $\alpha + \alpha + n$ decay channel of the state due to a threshold regime, the approximate factorization of the energy dependence of the final state wave function, and the quite sizable contribution of the outer region to the reaction cross section.

The model [5] provides potentials

$$V(r) = V_0/[1 + e^{(r-R)/b}] \quad (1)$$

describing $n - {}^8\text{Be}$ scattering. The best version

$$V_0 = 35.99 \text{ MeV}, \quad R = 3.126 \text{ fm}, \quad b = 0.8108 \text{ fm} \quad (2)$$

will be used below. Other potential versions lead to similar results as it is commented below.

Denote $E = (\hbar k)^2/(2\mu)$ the energy of the relative $n-{}^8\text{Be}$ motion. The potential (1), (2) leads to a $n-{}^8\text{Be}$ scattering amplitude $f(k)$ having a pole at $k = -i\kappa$, $\kappa > 0$:

$$f(k) \rightarrow \frac{iC}{k + i\kappa} \quad (3)$$

at $k \rightarrow -i\kappa$. This means that the first excited state of ${}^9\text{Be}$ is a virtual state strongly coupled to the $n-{}^8\text{Be}$ channel. The energy of the state is

$$-(\hbar\kappa)^2/(2\mu) = -\bar{E} = -23.53 \text{ KeV.} \quad (4)$$

This value was obtained via solving the eigenvalue problem with the virtual state boundary condition, cf. Appendix A.

Let us consider the shape of the line for a transition proceeding via the virtual state. The shape depends partly on a specific way of the excitation of the state. The "main" energy dependence is, universal however, and it is determined by the intrinsic properties of the state. We shall compare the universal energy dependence to the energy dependence for the process of photodisintegration of ${}^9\text{Be}$.

We assume that the cross section for formation of ${}^9\text{Be}$ in the continuum with the energy E in the vicinity of the excited level can approximately be presented in the form

$$\sigma \sim \int k^2 dk |\langle \Phi | \Psi_k (J = 1/2^+) \rangle|^2 \delta(k^2/(2\mu) - E) \quad (5)$$

Here Φ is some localized state in the subspace of ${}^9\text{Be}$ degrees of freedom. It may depend on energy being smooth at $E \rightarrow 0$. The function Ψ_k is the continuum spectrum function that corresponds to the colliding n and ${}^8\text{Be}$ fragments. The representation (5) implies that the formation process can be described in the subspace of ${}^9\text{Be}$ degrees of freedom. At such a condition properties of a state reveal themselves irrespective to interaction with other particles participating in its formation. Furthermore, in the function Ψ_k we retain only the elastic scattering channel and disregard the three-body $\alpha + \alpha + n$ breakup channels. Breakup components coupled to the excited state are relatively small due to the small energy. In Eq. (5) the normalization condition $\langle \Psi_k | \Psi_{k'} \rangle = \delta(k - k')/k^2$ should be fulfilled, so that the $n-{}^8\text{Be}$ relative motion function entering Ψ_k at large distances is normalized to $\sin(kr + \delta)/(kr)$. To describe the phase shifts δ we can use the potential (1), (2) derived from the analysis [5] of the total photodisintegration cross section because the direct $\alpha\alpha n$ disintegration cross section is presumably very small due to the threshold regime. The latter is confirmed in experiment, see [5].

The energy dependence of the cross section (5) in the vicinity of the virtual level is $\sin^2 \delta/k$. This energy dependence arises if one replaces the outer part $\sin(kr + \delta)/(kr)$ of the $n-{}^8\text{Be}$ relative motion function in the matrix element from Eq. (5) by $\sin \delta/(kr)$. This can be done under the conditions $(kR)^2 \ll 1$, and $R \ll a$. Here a is the scattering amplitude, and R is chosen such that the relative contribution of $r > R$ values to Eq. (5) is small. R exceeds the range of the $n-{}^8\text{Be}$ interaction, and the inner part of the final state wave function Ψ_k acquires the same energy dependence as the outer one. The $\sin^2 \delta/k$ energy dependence is nothing else as the so called Migdal-Watson factor [6].

We can rewrite the corresponding cross section as $\text{const} \cdot k |f(k)|^2$ where $f(k)$ is the s -wave $n-{}^8\text{Be}$ scattering amplitude. Almost the same accuracy is kept if one takes $f(k)$ within the effective range approximation

$$f(k) = [-1/a + (1/2)r_0k^2 - ik]^{-1}. \quad (6)$$

Then one obtains $|f(k)|^2 = [E + \bar{E})(E + E_1)]^{-1}$. In our case $E_1 = 1.569$ MeV. Using this expression, it is convenient to present the cross section in the following form

$$\sigma(E) = \sigma_m \frac{2\sqrt{E\bar{E}}}{E + \bar{E}} \frac{\bar{E} + E_1}{E + E_1}. \quad (7)$$

Since $\bar{E} \ll E_1$ the energy dependence of the cross section from the threshold up to its maximum is entirely determined by the second factor in Eq. (7). It is then seen that the maximum of the cross section occurs practically at the \bar{E} value. With a high precision σ_m is the value of the cross section at the maximum. As one can see from Eq. (5) the lowest order correction to Eq. (7) is of the form $1 - (E/E_2)$ where E_2 is not small and depends on a specific excitation process. To a certain degree it can be accounted for via a renormalization of E_1 . Eq. (5) is the Breit-Wigner formula with $\Gamma = \Gamma(E)$, (or, the one-level R matrix expression) rewritten in another form.

In Fig. 1 various universal expressions for the shape of the line are compared with the exact line shape for the photodisintegration process calculated in the model of Ref. [5]. ($E = E_\gamma - E_{th.}$) The full curve represents the latter cross section, the long-dashed curve is the energy dependence $\sim k|f(k)|^2$, the dash-dotted curve represents the expression (7), and the dotted curve is the energy dependence given by the second, i.e. resonant factor from Eq. (7). The FWHM value for the photodisintegration process provided by the first mentioned curve is 196 KeV. The FWHM values provided by the next two curves are 230 and 240 KeV. The latter two values are process-independent. Thus FWHM may depend rather sizably on the excitation process. On the contrary, the position of the maximum in the peak is practically process-independent coinciding with the absolute value of the energy of the virtual state.

Experimentally, the energy dependence $E^{1/2}(E + \bar{E})^{-1}$, specific to a virtual state could be confirmed by measuring the shape of the line from the threshold up to the region of the maximum with the tagged photon techniques. A simpler, while indirect, way is to study the whole peak in the (e, e') reaction and extract the properties of the state in the way similar to that used above for photodisintegration. In case of accurate and detailed (e, e') or (p, p') data the energy \bar{E} of the state could also be extracted from the fit of Eq. (7) form or its above-mentioned extension.

Besides the energy \bar{E} , or the pole position of the $n-{}^8\text{Be}$ scattering amplitude, another quantity to be reproduced in a microscopic calculation is the residue C in the pole, Eq. (3). The exact C value was calculated with the formula derived in Appendix A that represents C as an integral taken over the virtual state eigenfunction. The result is $C = 0.7837$. We note that both \bar{E} (or κ , see (4),) and C can be expressed in terms of the $n-{}^8\text{Be}$ scattering length a and the effective range r_0 with high accuracy. From Eq. (6) one obtains

$$\begin{aligned} \kappa &= r_0^{-1}[(1 - 2r_0/a)^{1/2} - 1], \\ C &= (1 - 2r_0/a)^{-1/2} = (1 + \kappa r_0)^{-1}. \end{aligned} \quad (8)$$

The effective range parameters for the potential (1), (2) are

$$a = -27.65 \text{ fm}, \quad r_0 = 8.788 \text{ fm}, \quad (9)$$

and the expected accuracy of the above expressions is about $(r_0/a)^3 \simeq 1\%$. Their numerical values proved to be even more accurate: $\bar{E} = 23.51$ KeV, $C = 0.7819$. As it is explained in [5] all other acceptable potentials found there lead to the a and r_0 values very close to those in Eq. (9). Hence the properties of the virtual state given by these potentials are quite similar.

III. THE FIRST EXCITED LEVEL OF ${}^9\text{B}$

To calculate the resonant peak for an excitation of the ${}^9\text{B}$ $1/2^+$ level, we proceed again from Eq. (5) assuming that the only decay channel for the state considered is $p-{}^8\text{Be}$. In the ${}^9\text{B}$ case, disregarding the possibility for decay into the $N + \alpha + \alpha$ channel, being less substantiated than in the ${}^9\text{Be}$ case because of higher energy with respect to the three-body threshold, seems still to be reasonable. The $n-{}^8\text{Be}$ potentials obtained in Ref. [5] lead presumably to a good description of the $n-{}^8\text{Be}$ $1/2^+$ phase shifts. Then one may suggest that the $p-{}^8\text{Be}$ $1/2^+$ phase shifts will also be properly reproduced with these potentials with an addition of the Coulomb interaction. This will suffice to obtain the main properties of the $1/2^+$ level.

Beyond the range of the nuclear potential the $p-{}^8\text{Be}$ relative motion function $\chi(r)/kr$ entering Ψ_k in Eq. (5) may be represented in the form

$$\chi = G \sin \delta + F \cos \delta = (\sin \delta/C)[C(G + F \cot \delta)] \equiv (\sin \delta/C)\phi(k, r). \quad (10)$$

Here δ is the nuclear phase shift, C^2 is the Coulomb penetrability factor (B1), and F and G are the Coulomb functions. The resonant pole is contained in the factor $\sin \delta$ while the function ϕ from Eq. (10) is smooth at small energies. (At $k \rightarrow 0$ $\phi(k, r) \rightarrow zK_1(z) - (a_c/4a)zI_1(z)$, $z = 2(2r/a_c)^{1/2}$, where a is the scattering length, and a_c is the Bohr radius.) To the first approximation one may use $\phi(k_0, r)$ at the calculation of the cross section (5), k_0 being chosen in the vicinity of the resonance. Hence the energy dependence of the excitation cross section in the resonant peak region is given by the expression¹

$$\frac{\sin^2 \delta}{kC^2} = k \frac{|f(k)|^2}{C^2} = \frac{kC^2}{(kC^2 \cot \delta)^2 + (kC^2)^2}. \quad (11)$$

Here f is the amplitude of $p-{}^8\text{Be}$ scattering. Thus, quite naturally, the resonant cross section for the excitation of the state is proportional to the scattering cross section times a factor which is a universal one up to corrections proportional to a width. Those corrections are process-dependent. The quantity $kC^2 \cot \delta$ in (11) allows the well-known presentation [7] $[-1/a + (1/2)r_0k^2 + \dots] - (2/a_c)h(1/a_ck)$, cf. Appendix B, showing that it is smooth and finite at $E = 0$. The kC^2 behavior of the cross section at $E \rightarrow 0$ is seen directly from Eq. (5) and the properties of the Coulomb functions.

The $p-{}^8\text{Be}$ phase shifts entering Eq. (11) were obtained from the Schrödinger equation with the nuclear potential (1), (2) plus the Coulomb interaction. The latter took into account the density distribution in ${}^8\text{Be}$ and the charge distribution in the α particles:

¹It might be that this expression was already used by someone, and we do not claim the opposite.

$$V_{Coul}(r) = (4e^2/r)(2/\pi) \int_0^\infty (\sin qr/q) F_\alpha(q) I(q) dq, \quad (12)$$

where $F_\alpha(q)$ is the charge form factor of the α particle [8], and

$$I(q) = \int_0^\infty (2/q\rho) \sin(q\rho/2) \psi^2(\rho) d\rho,$$

ψ being the ${}^8\text{Be}$ wave function.

The resonant energy dependence (11) obtained is shown in Fig. 2 with a solid curve. The position E_{max} of the maximum in the peak with respect to the $p-{}^8\text{Be}$ threshold and the FWHM value are the following: $E_{max} = 1.13$ MeV, FWHM = 1.64 MeV. The long-dashed curve in Fig. 2 represents the resonant peak for the other acceptable nuclear potential of the Woods-Saxon form found in Ref. [5] whose parameters are

$$V_0 = 52.86 \text{ MeV}, \quad R = 2.006 \text{ fm}, \quad b = 1.051 \text{ fm}. \quad (13)$$

For this case $E_{max} = 1.02$ MeV, and FWHM = 1.43 MeV.

Of interest is the energy eigenvalue pertaining to a resonant state. One can show, see Appendix B, that when the long-range Coulomb interaction is switched on virtual states cease to exist turning normally to complex-energy resonances, and this applies to our case. The energy $E = E_0 - i\Gamma/2$ of a resonance being connected to the pole of a scattering amplitude, is process-independent and thus characterizes a resonance quite precisely even in case of a broad width. In our case this quantity is computed as a complex eigenvalue from the $p-{}^8\text{Be}$ Schrödinger equation with the procedure described in Appendix C. The results are $E_0 = 0.60$ MeV, $\Gamma/2 = 0.77$ MeV, and $E_0 = 0.56$ MeV, $\Gamma/2 = 0.70$ MeV for the potentials (2) and (13), respectively. The positions E_0 of the resonance are shifted downwards with respect to the maxima in the peak found above, while the widths Γ are close to the FWHM values. Similar trends were observed for ${}^5\text{He}$, ${}^5\text{Li}$ resonances [9]. It is interesting to note that the height of the Coulomb barrier in our case proved to be 0.63 MeV only, i.e. the resonance sits at the top of the barrier. It is possible only due to a broad width of the resonance being comparable to E_0 .

It would be nice to extract the E_0 and Γ values from experimental data. For this purpose fits "adequate" for an extrapolation of data to the complex pole are required. One possibility connected to Eq. (11) is

$$A \frac{kC}{a + b(E - E')^2 + kC^2}$$

where A , a , b , and E' are fitting parameters. The $E_0 - i\Gamma/2$ value is the energy corresponding to the pole of the denominator of this expression.

In conclusion, let us comment on the value of the effective range r_0 for the $p-{}^8\text{Be}$ scattering. For the potential (2), for example, its value proved to be 3.01 fm i.e. much smaller than that from Eq. (9) for the $n-{}^8\text{Be}$ case. This, however, does not mean that the range of the $p-{}^8\text{Be}$ nuclear interaction is sizably different from that for the $n-{}^8\text{Be}$ interaction. The effective range can serve as a measure of the interaction range when $a \gg r_0$ and, in addition, the zero energy scattering wave function $u(r)$ entering the effective range definition is close to unity at the edge of the well R . This holds true for the neutral case but not when the rather strong Coulomb interaction is present. The latter interaction suppresses the wave function at the R value, so that the range of nuclear interaction may be estimated as $r_0/u^2(R)$.

IV. DISCUSSION

Basing on the model of Ref. [5] we obtained that the first excited level of ${}^9\text{Be}$ is a virtual state with the energy $-\bar{E} = -23.5$ KeV with respect to the $n-{}^9\text{Be}$ threshold. It was shown that the peak position for an excitation of this state practically coincides with the \bar{E} value while the FWHM value of the peak may sizably depend on the specific excitation process. Within the effective range approximation the properties of the state are reproduced with a high accuracy.

In Ref. [10] it was obtained from a single-level R -matrix fit to the photodisintegration data of Ref. [11] that the state considered is a complex-energy resonant state. However the data [11] are at variance with the earlier data, and it was concluded in Ref. [5] that the latter ones are preferable. The positions of maxima in the available experimental ${}^9\text{Be}(p, p')$ spectra [12,13] do not contradict to the above listed value of 23.5 KeV.

In Ref. [13] the quantities pertaining to the $1/2^+$ state of ${}^9\text{Be}$ were presented in the form of parameters entering the Breit-Wigner formula

$$\sigma(E) = \frac{8\pi^2 e^2}{9 \hbar c} E_\gamma B(E1, E_\gamma) \frac{\Gamma(E)}{(E - E_R)^2 + [\Gamma(E)]^2}, \quad (14)$$

that was fitted to the (e, e') data of that paper. Here $\Gamma(E) = G\sqrt{E}$, G being the reduced width of the level. The values $E_R = 19 \pm 7$ KeV, $\Gamma = 217 \pm 10$ KeV were listed, the latter value refers presumably to $\Gamma(E_R)$. These values are quoted in the review article [14]. They cannot be correct since they lead to a quite unrealistic \bar{E} value, i.e. that of the maximum of an excitation cross section, of 0.6 KeV. Basing on Fig. 6 from Ref. [13] one may suggest, however, that these values should be referred not to E_R and Γ from Eq. (14) but to the position of the maximum of the cross section and the FWHM, respectively. If it is the case, these values are in agreement with ours. (Absence of information on the energy dependence of $B(E1, E_\gamma)$ inhibits a precise conclusion concerning the FWHM.)

In Ref. [2] a microscopic study of the spectrum of ${}^9\text{Be}$ at the 9-nucleon level has been undertaken. The $1/2^+$ level has not been detected at all. The reason may lie in that the method of complex scaling used in that work is suited for search of complex-energy resonant states but not virtual states.

Using the nuclear potentials derived in [5] from the analysis of the ${}^9\text{Be}$ photodisintegration data and adding the Coulomb interaction between p and ${}^8\text{Be}$, we studied the first excited state in ${}^9\text{B}$. An approximate process-independent expression describing the peak of the resonance in the excitation cross section has been obtained. The position of the peak with respect to the $p-{}^8\text{Be}$ threshold and its FWHM given by this expression are about 1.1 MeV and 1.5 MeV, respectively. The peak considered is caused by a complex-energy pole in the $p-{}^8\text{Be}$ scattering amplitude. The pole proved to be located at energy $E = E_0 - i\Gamma/2$ with $E_0 \simeq 0.6$ MeV and $\Gamma \simeq 1.5$ MeV.

In addition to the omission of the three-body breakup channel in the $p-{}^8\text{Be}$ scattering wave function, our study of the ${}^9\text{B}$ resonance has two main limitations. First, according to Eq. (11) the line shape is determined by the $p-{}^8\text{B}$ phase shifts. These phase shifts have been obtained from two-body $p-{}^8\text{Be}$ dynamics that do not describe explicitly the distortion of ${}^8\text{Be}$ in the interaction region. In this connection one should first discuss the status of the $n-{}^8\text{B}$ potentials we use. The 60-70% contribution to the photodisintegration cross

section described with this potentials comes from an exterior region, and this contribution is directly determined by $n-{}^8\text{Be}$ phase shifts. At small E , the energy dependence of the rest contribution is also determined mainly by the same phase shifts irrespective to the distortion of ${}^8\text{Be}$ in the interior region. Therefore, one can think that the $n-{}^8\text{Be}$ low-energy scattering parameters and thus the $n-{}^8\text{Be}$ phase shifts in a considerable energy range are derived correctly from the data. Hopefully, one comes to approximately correct $p-{}^8\text{B}$ phase shifts as well when adding the Coulomb interaction to the potentials thus obtained. (The Coulomb interaction is important mostly in the exterior region where no strong distortion of ${}^8\text{Be}$ occurs.) The second limitation consists in the neglection of a change with energy of the function $\phi(k, r)$ in Eq. (10). Since the resonance is broad this approximation might be not very accurate. This limitation is avoided if one compares the resonance eigenenergy $E_0 - i\Gamma/2$ with experiment. On the other hand, in view of the said below the limitation might be not very serious.

In Ref. [3] a prediction for the peak of the ${}^9\text{B}$ resonance was obtained: $E_{max} = 1.13$ MeV, FWHM=1.40 MeV. It is close to ours while the underlying assumptions of that work were rather different. Our common features with that work consist in use of $p-{}^8\text{Be}$ dynamics to obtain the resonance and in obtaining the $p-{}^8\text{Be}$ Woods-Saxon potential from ${}^9\text{Be}$ photodisintegration data. The differences consist in a way to deduce the parameters of the potential, in the parameters themselves, and in a prescription to calculate the resonance. In Ref. [3] the two-body dynamics were used both for the initial ground state and the final continuum state of ${}^9\text{Be}$. Depths of the potentials were varied whereas their range and diffuseness were kept at their "classic" values. The data of Ref. [11] were fitted (probably up to a normalization). The fit was only moderately good. The line shape of the ${}^9\text{B}$ resonance was computed as if it was excited due to a fictitious dipole transition from the ground state of ${}^9\text{Be}$. Our potentials were derived [5] at the assumption of three-body $\alpha + \alpha + n$ dynamics for the ground state of ${}^9\text{Be}$ and two-body dynamics for its continuum. Range and diffuseness of the potential were varied in addition to the depth. The data of Ref. [11] were concluded to be less preferable, and the alternative earlier data were fitted without freedom in an absolute normalization. The fit is statistically quite good. The line shape of the ${}^9\text{B}$ resonance was computed from Eq. (11). The Coulomb interaction was treated more accurately, and also the pole position $E_0 - i\Gamma/2$ was calculated. Keeping range and diffuseness of the potential at their "classic" values was perhaps an important point in the analysis of Ref. [3] which allowed obtaining correct results even at assumptions that are not completely valid. An interesting point is that the different prescriptions for calculating a resonance in our work and in Ref. [3] lead to similar results. To check this we calculated the resonance for the potential of Ref. [3] with the prescription of Eq. (11). The results are $E_{max} = 1.06$ MeV, FWHM=1.47 MeV, and they are close to those reported in Ref. [3]. (A difference in treatment of the Coulomb interaction should also be taken into account here.)

In Ref. [15] the energy of the $1/2^+$ first excited state of ${}^9\text{B}$ was derived from R -matrix parameters fitted [10] to the ${}^9\text{Be}$ data of Ref. [11] and from values of the Coulomb displacement energy calculated with the help of the shell model. The result $E_0 \simeq 2$ MeV differs considerably from that of our work and Ref. [3] leading to the inverted value of the so called Thomas-Ehrmann shift. Use of the particular set of data to derive R -matrix parameters might be a disadvantage.

We are indebted to M.V. Zhukov for useful conversations in the course of this study.

A part of this work was done during the stay of V.D.E. at the Niels Bohr Institute, and he expresses his gratitude for the kind hospitality. The work was partially supported by Russian Foundation for Basic Research (grants 96-15-96548 and 97-02-17003).

APPENDIX A: RESIDUE PROPERTIES OF VIRTUAL STATE POLES OF A SCATTERING AMPLITUDE

We obtain a formula that expresses a residue at a virtual state pole in terms of a quadrature taken over the virtual state eigenfunction. The consideration is formally applicable to motion in a central potential with any orbital momentum l although the $l > 0$ virtual state case is of little interest.

Let $\psi(r)$ be the solution to the Schrödinger equation regular at the origin. Beyond the range of a potential $\chi(r) = r\psi(r)$ behaves as $(-1)^l S^{-1}(k) \exp(-ikr) - \exp(ikr)$. Complex k values are allowed. A virtual state corresponds to a pole of the S -matrix $S(k)$ at $k = -i\kappa$, κ being real and positive.² In terms of κ , $\chi(r) = (-1)^l S^{-1} \exp(-\kappa r) - \exp(\kappa r)$ at large r , so the boundary condition for virtual states consists in absence of the decreasing exponential. If the eigenvalue is sufficiently small then the eigensolution can be found directly using a logarithmic derivative at large r . This holds true in our case.

Let us express a residue at the virtual state pole of a scattering amplitude in terms of the eigenfunction pertaining to a virtual state. The well-known corresponding formula for bound states [16,17] is the following. Let the bound state wave function be normalized to unity, and A be the coefficient in its asymptotics $A \exp(-\kappa r)$. Then

$$f(k) \rightarrow \frac{i(-1)^l A^2}{2\kappa} \frac{1}{k - i\kappa} \quad (\text{A1})$$

as k tends to $i\kappa$.

In the virtual state case we shall proceed from the relation

$$\frac{\partial\chi}{\partial r} \frac{\partial\chi}{\partial E} - \chi \frac{\partial^2\chi}{\partial r \partial E} = \frac{2m}{\hbar^2} \int_0^r \chi^2(r') dr'. \quad (\text{A2})$$

It is similar to that used in Ref. [6] for the derivation of Eq. (A1). We take r to be large enough so that in the vicinity of the virtual state pole $\chi \simeq \exp(\kappa r) + \alpha(E + \bar{E}) \exp(-\kappa r)$. Here $\bar{E} = (\hbar\kappa)^2/2m$. The pole term in the scattering amplitude is then $(-1)^{l+1}(2\kappa\alpha)^{-1}(E + \bar{E})^{-1}$ and the parameter α is to be found. We set

$$\chi_v(r) = \exp(\kappa r) + \Delta(r), \quad (\text{A3})$$

substitute this into the right-hand side of Eq. (A2) and equate the terms of the orders of $\exp(\kappa r)$ and unity in both sides of Eq. (A2) at E tending to $-\bar{E}$. Then we obtain $2\kappa\alpha = -(2m/\hbar^2)(I_v/2\kappa)$, with

$$I_v = 1 - 2\kappa \int_0^\infty [\Delta^2 + 2\Delta \exp(\kappa r)] dr. \quad (\text{A4})$$

²It is implied that at large r the potential decreases more rapidly than $\exp(-\kappa r)$, cf [6].

The function $\Delta(r)$ entering Eq. (A4) is a rapidly decreasing function since χ_v from Eq. (A3) is the eigenfunction. So the integral converges. Finally,

$$f(k) \rightarrow \frac{i(-1)^l}{I_v} \frac{1}{k + i\kappa} \quad (A5)$$

as k tends to $-i\kappa$, $\kappa > 0$.

To display an analogy between the bound and virtual state pole cases, we note that the right-hand side of Eq. (A1) can be rewritten as

$$\frac{i(-1)^l}{2\kappa N_b} \frac{1}{k - i\kappa}, \quad (A6)$$

where N_b is the norm integral for the eigenfunction χ_b normalized to $\exp(-\kappa r)$ as r tends to infinity. If one sets $\chi_b(r) = \exp(-\kappa r) + \Delta(r)$ then $2\kappa N_b$ takes just the form of Eq. (A4) with the replacement $\kappa \rightarrow -\kappa$.

APPENDIX B: ABSENCE OF VIRTUAL STATES// FOR POTENTIALS WITH THE COULOMB ASYMPTOTICS

We consider potentials with the Coulomb repulsive tail for $l = 0$ and energies within a limited range specified below. The scattering amplitude is $f_{coul} + \exp(i\phi_{coul})f_{nucl}$, where f_{coul} and ϕ_{coul} are the pure Coulomb amplitude and phase shift. Possible poles of the nuclear scattering amplitude f_{nucl} have to be considered. The amplitude is of the form $[k \cot \delta_{nucl} - ik]^{-1}$. As is well known, the quantity $k \cot \delta_{nucl}$ may be represented as $C^{-2}[K(k^2) - (2/a_c)h(\eta)]$ where a_c is the Bohr radius, C^2 is the penetrability factor,

$$C^2 = 2\pi\eta(\exp(2\pi\eta) - 1)^{-1} \quad (B1)$$

with $\eta = 1/(a_c k)$,

$$h(\eta) = \eta^2 \sum_{n=1}^{\infty} n^{-1} (n^2 + \eta^2)^{-1} - \ln \eta - \gamma, \quad (B2)$$

and $K(z)$ is a function analytic at $z = 0$. We consider energies within the range of analyticity of this function. Normally, this range exceeds several MeV. Since virtual states with small energies are of only interest this restriction is not a serious one. The equation to determine the poles of f_{nucl} is thus

$$K(k^2) - (2/a_c)h(\eta) = ikC^2. \quad (B3)$$

For the bound-state case one sets $k = i\kappa$, $\kappa > 0$. Then one uses Eq. (B1) and Eq. (B2) substituting $i[\exp(2iz) - 1]^{-1} = 1/2(-i + \cot z)$, and $\ln \eta = \ln(1/a_c \kappa) - i\pi/2$. The function $K(z)$ is real for real positive or negative z . As a result, imaginary parts in both sides of Eq. (B3) cancel, and one obtains the real equation [7] to determine bound state energies:

$$K(-\kappa^2) - (2/a_c)[-s^2 \sum_{n=1}^{\infty} n^{-1} (n^2 - s^2)^{-1} - \ln s - \gamma] = -(\pi/a_c) \cot(\pi s), \quad (B4)$$

with $s = (a_c \kappa)^{-1}$. (Note that the singularities at s being integer cancel in Eq. (B4).)

In the virtual state case $k = -i\kappa$, $\kappa > 0$, one comes instead to the equation

$$K(-\kappa^2) - (2/a_c)[-s^2 \sum_{n=1}^{\infty} n^{-1} (n^2 - s^2)^{-1} - \ln s - \gamma] + (i\pi/a_c) = -(i\pi/a_c) + (\pi/a_c) \cot(\pi s)$$

that includes an imaginary constant and thus has no solutions. Hence, virtual levels cannot exist in the case considered.

According to the said above the low-energy level in the pp system, for example, is not a virtual level, as sometimes claimed, but a complex energy resonant level. The calculation in the framework of the effective range approximation for the pp scattering amplitude gives $E_0 = -0.143$ MeV, $\Gamma/2 = 0.468$ MeV for its energy. E_0 is negative, so it is not a conventional resonance.

APPENDIX C: CALCULATION OF RESONANT EIGENSTATES

The following way to solve the eigenvalue problem for resonances proved to be convenient. We integrate the Schrödinger equation for $\chi(r) = r\psi(r)$ downwards starting at some point $r = R$ that lies beyond the range of a nuclear potential. The outgoing wave boundary condition $\chi = G(\rho, \eta) + iF(\rho, \eta)$, $d\chi/dr = k[G'(\rho, \eta) + iF'(\rho, \eta)]$ where G and F are the Coulomb functions [18], is imposed at $r = R$. The χ value at the origin thus obtained depends on the trial complex energy, or wavenumber $k = k_1 + ik_2$. One should require $\chi(r = 0, k) = 0$ that gives a transcendental equation of the type $f(k) = 0$ to determine the energy of the resonance. To solve it one can apply the Newton type procedure, for example: $k_{n+1} = k_n - f(k)/g(k)$, $g(k) = [f(k + \delta) - f(k - \delta)]/(2\delta)$, δ being a small increment. The k value obtained from E_{max} and FWHM may usually serve as an initial approximation. The complex energy Schrödinger equation is thus solved within a not too large range of r values that allows obtaining an accurate solution. In our case use of R value as small as 12 fm allows the determination of the eigenvalue $E = E_0 - i\Gamma/2$ with the accuracy in 0.001 MeV.

The procedure requires the calculation of the Coulomb functions and their derivatives at complex ρ and η values, and the results are sensitive to the accuracy of the calculation. We used for this purpose the computer codes of Ref. [19]. The results were checked with the asymptotic estimate for $G + iF$. However we failed to use them for $R > 17$ fm. Besides, the codes may require adjustments to a given computer type. A convenient procedure alternative to that used in [19] is the following. The function F is found as a series expansion: $F = C\rho\Phi(\eta, \rho)$, $\Phi = \sum_{k=1}^{\infty} A_k(\eta)\rho^{k-1}$. The expansion coefficients are obtained with the recursion relation [18]. The function G is calculated with the formula listed in [18]. We rewrite it for $l = 0$ in the form valid for complex η values:

$$G(\eta, \rho) = C^{-1} \left\{ 2\eta\rho\Phi(\eta, \rho) [\ln(2\rho) + y(\eta)] + \sum_{k=0}^{\infty} a_k(\eta)\rho^k \right\}$$

The expansion coefficients are obtained with the help of the recursion relation listed in [18], and

$$y(\eta) = (1/2)[\psi(i\eta) + \psi(-i\eta)] + 2\gamma - 1 = \gamma - 1 + \eta^2 \sum_{n=1}^{\infty} n^{-1} (n^2 + \eta^2)^{-1}.$$

Here $\psi(z) = \Gamma'(z)/\Gamma(z)$, and γ is the Euler constant. The coefficients of the series expansions entering the expressions for both F and G decrease as $(k!)^{-1}$ or faster so the expansions are rapidly convergent for not extremely high $|\rho|$ or $|\eta|$ values.

REFERENCES

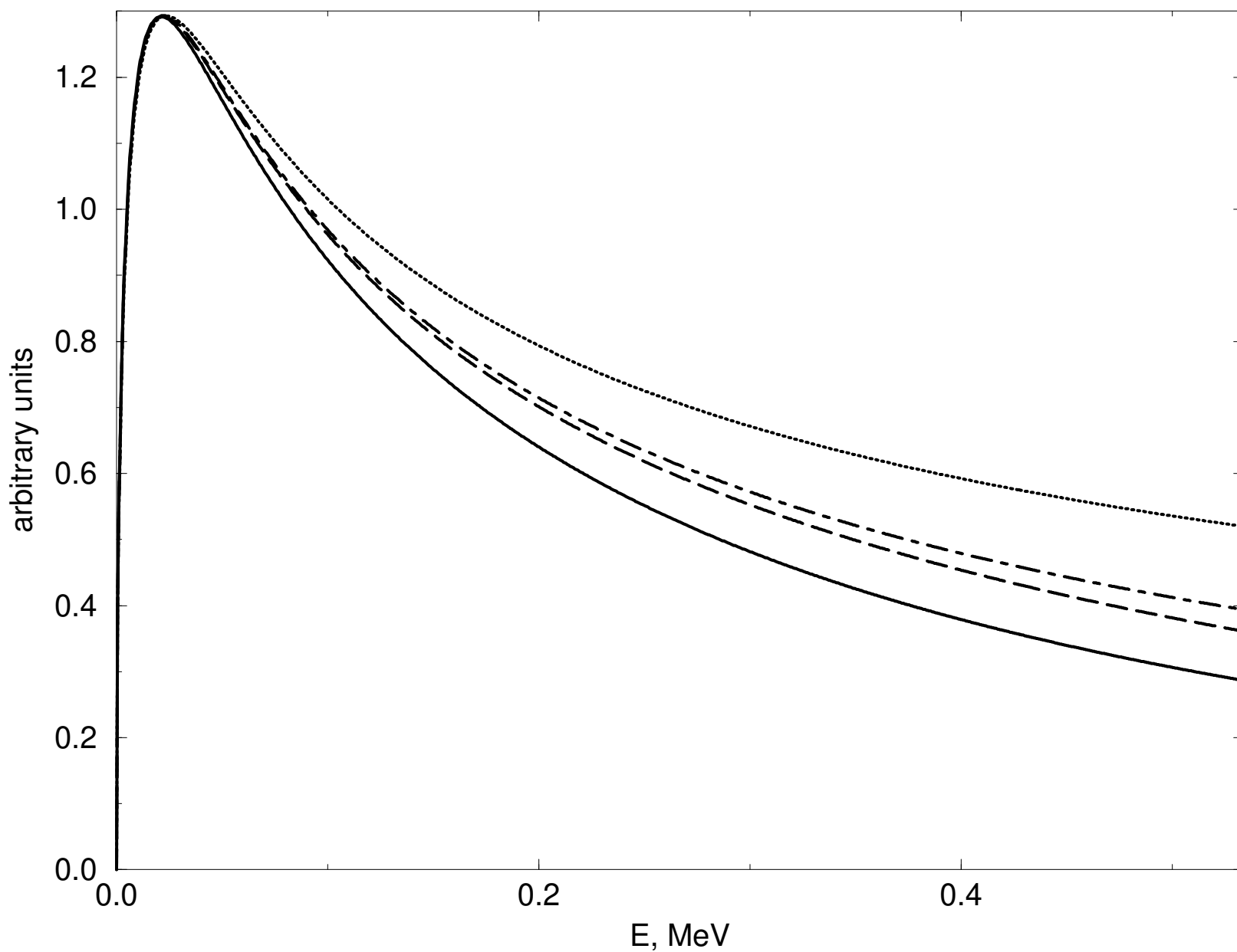
- [1] V.T. Voronchev, V.I. Kukulin, V.N. Pomerantsev, and G.G. Ryzhikh, Few-Body Sys. **18**, 1995.
- [2] K. Arai, Y. Ogawa, Y. Suzuki, and K. Varga, Phys. Rev. C **54**, 132 (1996).
- [3] R. Sherr and G. Bertsch, Phys. Rev. C **32**, 1809 (1985).
- [4] M.A. Tiede et al., Phys. Rev. C **52**, 1315 (1995); F.C. Barker, Phys. Rev. C **53**, 2539 (1996).
- [5] V.D. Efros, H. Oberhummer, A.V. Pushkin, and I.J. Thompson, Europ. Phys. J. 1998 (in press).
- [6] L.D. Landau and E.M. Lifshitz, Quantum Mechanics, Pergamon 1977.
- [7] L.D. Landau and Ya.A. Smorodinsky, J. Phys. (USSR) **8**, 154 (1944), reprinted in: L.D. Landau, Collected papers, D. ter Haar ed., Oxford, Pergamon Press, 1965.
- [8] C.R. Ottermann et al., Nucl. Phys. **A436**, 688 (1985).
- [9] V.D. Efros and H. Oberhummer, Phys. Rev. C **54**, 1485 (1996).
- [10] F.C. Barker, Can. J. Phys. **61**, 1371 (1983).
- [11] M. Fushiro et al. Can. J. Phys. **60**, 1672 (1982).
- [12] S.N. Tucker, P.B. Treacy, and V.V. Komarov, Aust. J. Phys. **23**, 651 (1970).
- [13] G. Kuechler, A. Richter, and W. von Witsch, Z. Phys. **A326**, 447 (1987).
- [14] F. Ajzenberg-Selove, Nucl. Phys. **A490**, 1 (1988).
- [15] F.C. Barker, Aust. J. Phys. **40**, 307 (1987).
- [16] H.A. Kramers, Hand und Jahrbuch der Chemisher Physik **1**, 312 (1938).
- [17] W. Heisenberg, Z. Naturforsh. **1**, 608 (1946); C. Möller, Dan. Vid. Selsk. Mat. Phys. Medd. **22**, N19 (1946); N. Hu, Phys. Pev. **74**, 131 (1948).
- [18] M. Abramovitz and I.A. Stegun, Handbook of Mathematical Functions, Dover, N.Y., 1970.
- [19] I.J. Thompson and A.R. Barnett, Comp. Phys. Com. **36**, 363 (1985).

FIGURES

FIG. 1. Line shapes for transitions to the first excited state of ${}^9\text{Be}$. The solid curve represents the exact line shape for the photodisintegration process calculated with the model of Ref. [5]. The long-dashed curve is the energy dependence $k|f(k)|^2$, where f is the $n-{}^8\text{Be}$ scattering amplitude. The dash-dotted curve stands for Eq. (7). The dotted curve represents the energy dependence given by the second factor from Eq. (7).

FIG. 2. Line shapes for transitions to the first excited state of ${}^9\text{B}$ calculated according to Eq. (11). The solid and long-dashed curves are for the potentials with the parameters (2) and (13), respectively.

9Be 1/2+



9B 1/2+

